



This is the accepted manuscript made available via CHORUS, the article has been published as:

Far-from-Equilibrium Quantum Magnetism with Ultracold Polar Molecules

Kaden R. A. Hazzard, Salvatore R. Manmana, Michael Foss-Feig, and Ana Maria Rey
Phys. Rev. Lett. **110**, 075301 — Published 11 February 2013

DOI: [10.1103/PhysRevLett.110.075301](https://doi.org/10.1103/PhysRevLett.110.075301)

Far from equilibrium quantum magnetism with ultracold polar molecules

Kaden R. A. Hazzard,* Salvatore R. Manmana, Michael Foss-Feig, and Ana Maria Rey
JILA, NIST, and Department of Physics, University of Colorado-Boulder, Boulder, Colorado 80309-0440, USA

Recent theory has indicated how to emulate tunable models of quantum magnetism with ultracold polar molecules. Here we show that *present* molecule optical lattice experiments can accomplish three crucial goals for quantum emulation, despite currently being well below unit filling and *not* quantum degenerate. The first is to verify and benchmark the models proposed to describe these systems. The second is to prepare correlated and possibly useful states in well-understood regimes. The third is to explore many-body physics inaccessible to existing theoretical techniques. Our proposal relies on a non-equilibrium protocol that can be viewed either as Ramsey spectroscopy or an interaction quench. The proposal uses only routine experimental tools available in any ultracold molecule experiment. To obtain a global understanding of the behavior, we treat short times perturbatively, develop analytic techniques to treat the Ising interaction limit, and apply t-DMRG to disordered systems with long range interactions.

PACS numbers: 67.85.-d,75.10.Jm,71.10.Fd,33.80.-b

Excitement about the recent achievement of near-degenerate ultracold polar molecules [1–5] in optical lattices [6] stems from their strong dipolar interactions and rich internal structure, including rotational, vibrational, and hyperfine states. These features may be applied to tests of fundamental constants [7], quantum information [8], ultracold chemistry [9], and quantum emulation of condensed matter models [10–12]. In this paper our focus is on molecules as emulators of quantum magnetism [13–25], specifically as proposed in Refs. [26, 27]. Models of quantum magnetism have some of the simplest many-body Hamiltonians, yet describe numerous materials [28–30] and display condensed matter phases ranging from fundamental to exotic: antiferromagnets, valence bond solids, symmetry protected topological phases, and spin liquids. Emulating quantum magnetism with molecules is appealing because, like cold atoms, the systems are clean and the microscopics well understood. Advantages over cold atom emulations of quantum magnetism [31] include orders of magnitude larger energy scales and more tunable Hamiltonians [26, 27]. These prior studies have focused on spin *ground states* of unit filling insulators. In contrast, we propose a simple *dynamic* procedure applicable to present experiments (Fig. 1, elaborated later), which are ultracold, but non-degenerate and low density. We show that interesting many body quantum magnetism can be studied immediately.

Specifically we show how experiments may use this dynamics to achieve major goals for emulating quantum magnetism, and we outline these goals to motivate our calculations. First, although interesting models of quantum magnetism are predicted to describe ultracold molecules under appropriate circumstances, this has yet to be experimentally demonstrated. The proposed dynamic protocol allows such a demonstration as well as benchmarking of the emulator’s accuracy. Second, one wishes to prepare interesting correlated — and possibly

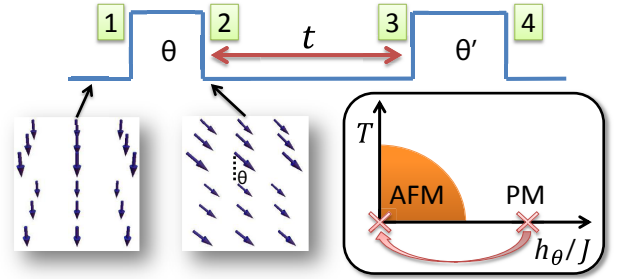


FIG. 1. (Color online) Dynamic protocol viewed as Ramsey spectroscopy, two microwave pulses of area θ and θ' separated by time t . Inset: alternative view as an interaction quench, a $t = 0$ sudden turn-off of an infinite strength field h_θ along θ .

useful — states. This protocol can generate such states in well-understood regimes. Finally, one wants to explore behavior in these models in regimes inaccessible to present theoretical tools. This is the generic case for the proposed dynamics. We emphasize that all of these goals are achievable under *existing* experimental conditions [6], despite present experiments being *non*-quantum degenerate and at low density. Furthermore, they require only routinely used measurement and preparation tools [32].

Background.—Refs. [26, 27] show how molecule rotational states can serve as effective spins, and that dipolar interactions provide an effective spin-spin interaction. In the simplest case, one populates two rotational levels in a dc electric field \mathbf{E} [33] and works in a deep lattice to allow no tunneling. In this limit, a spin-1/2 dipolar quantum XXZ model describes the molecules [34]:

$$H = \frac{1}{2} \sum_{i \neq j} V_{\text{dd}}(i, j) \left[J_z S_i^z S_j^z + \frac{J_\perp}{2} (S_i^+ S_j^- + \text{H.c.}) \right]. \quad (1)$$

The sum runs over all molecules, S_i^z and S_i^\pm are the spin-1/2 operators satisfying $[S_i^z, S_i^\pm] = \pm S_i^\pm$, and $V_{\text{dd}}(i, j) = (1 - 3 \cos^2 \Theta_{ij}) / |\mathbf{r}_i - \mathbf{r}_j|^3$ with \mathbf{r}_i the i 'th molecule's po-

sition in lattice units and Θ_{ij} the angle between \mathbf{E} and $\mathbf{r}_i - \mathbf{r}_j$. For simplicity and concreteness we assume a dimension $d \leq 2$ system with \mathbf{E} perpendicular to it, so $V_{\text{dd}}(i, j) = 1/|\mathbf{r}_i - \mathbf{r}_j|^3$, but our ideas apply in arbitrary geometries. One may tune J_{\perp}/J_z by changing \mathbf{E} and the choice of rotational state. We denote by $|0\rangle$, $|1\rangle$, and $|2\rangle$ the three lowest energy rotational eigenstates in the applied \mathbf{E} -field with zero angular momentum along the quantization axis. Choosing $|0\rangle$ and $|1\rangle$ to make the spin-1/2, one can tune $\infty > J_{\perp}/J_z > 0.35$ using (readily achievable) \mathbf{E} -fields from 0 to 16 kV/cm. Choosing $|0\rangle$ and $|2\rangle$ for the spin-1/2, one can tune $0 < J_{\perp}/J_z < 0.1$ for similar \mathbf{E} -fields. Fig. 2 shows the couplings' E -field dependence for these rotational level choices in both natural units ($d_p =$ permanent dipole moment and $B =$ rotational constant) and real units for KRB in a 532 nm lattice. A characteristic scale for these couplings is 400 Hz in KRB and 40 kHz in LiCs [35], compared to $\lesssim 10$ Hz in cold atoms using superexchange [36] (we set $\hbar = 1$). KRB molecules recently have been loaded in a deep three-dimensional lattice with 25 s lifetimes [6], allowing dynamics lasting thousands of J_{\perp}^{-1} and J_z^{-1} .

One important aspect of the ongoing experiments is that the filling f is much less than one molecule per site. The JILA experiments estimate $f \sim 0.1$ [37]. As a result, although molecules are static through one shot, they fluctuate shot-to-shot. Thus, rather than forming a regular lattice, spins' locations have significant disorder.

We use a simple disorder model that likely describes current experiments. We assume that each site is occupied with a probability p that is independent of other sites [38]. If the molecules are fermions (e.g., KRB [6]) then for current temperatures, which occupy only the lowest band, no sites can be doubly occupied and $p = f$. This also applies to bosons with a strong on-site density-density interaction (e.g., RbCs [39]). The trap causes f to vary spatially. Although we show results only for the homogeneous system, we have taken the trap into account and found that our conclusions remain valid [40]. Remarkably, relatives of such unusual models exist, and are employed to understand materials, ^3He - ^4He mixtures, and disorder-induced phenomena [41–49].

Disorder is related to temperature, but one must distinguish motional temperature from spin temperature. Only through “disorder” does motional temperature enter, because the deep lattice freezes out the motion. Even if motional temperature is large it is entirely captured by the disorder. Experimental microwave manipulation can produce essentially zero *entropy* non-thermal spin states. While one could worry that disorder washes out the behavior, we will show that strong correlations, entanglement, and interesting many body physics survive large amounts of disorder.

Dynamic protocol.—Our dynamic procedure may be alternatively viewed as Ramsey spectroscopy or an interaction quench (Fig. 1). Ref. [50] studied closely re-

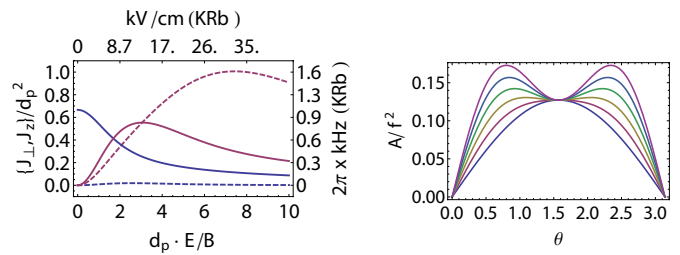


FIG. 2. (Color online) Left: DC electric field dependence of coupling constants J_{\perp} (blue) and J_z (purple) for $\{|0\rangle, |1\rangle\}$ (solid) and $\{|0\rangle, |2\rangle\}$ (dashed) rotational level choices to represent the spin-1/2. Top to bottom, at $E = 0$, these are J_{\perp}^1 , J_z^1 , J_z^2 , J_{\perp}^2 where superscript 1 and 2 denote the first and second choice of states, respectively. Units for KRB are in a 532 nm lattice. Right: rescaled short time coefficient A/f^2 , defined by $\langle S_i^x(t) \rangle = \langle S_i^x(0) \rangle - A\tau^2 + O(t^4)$, for a one dimensional dipolar chain, for fillings $f = 0, 0.2, \dots, 1.0$, bottom to top, with $\tau \equiv (J_z - J_{\perp})t$. Results are from Eqs. (2).

lated Rabi spectroscopy. In Ramsey spectroscopy, a well established tool in atomic physics, one begins with all molecules in the rotational ground state and applies two strong, resonant microwave pulses separated by time t . The first pulse initializes the spin states along θ , specifically to $\cos(\theta/2)e^{i\varphi/2}|\downarrow\rangle + \sin(\theta/2)e^{-i\varphi/2}|\uparrow\rangle$, for an angle θ set by the pulse area, with high fidelity ($> 99\%$). We take $\varphi = 0$ with no loss of generality. The second pulse rotates a desired spin component, chosen by the pulse area and phase, to the z axis. In this way one can measure any desired collective spin component $\langle \hat{n} \cdot \mathbf{S} \rangle$, where \hat{n} is a unit vector and $S^\alpha = \sum_i S_i^\alpha$ with $\alpha \in \{x, y, z\}$. One can also obtain higher moment correlations, e.g. $\langle (\hat{n} \cdot \mathbf{S})^2 \rangle$, from the measurement record. Between these pulses the spins evolve for a time t under the Hamiltonian in Eq. (1). We note that molecule experiments have recently begun using this protocol [32] and Ref. [51] applied it to long-range Ising models in recent Penning trap experiments with ~ 300 ions.

If one imagines adding a transverse field $h\mathbf{S} \cdot \hat{n}_\theta$ to Eq. (1)’s Hamiltonian, with \hat{n}_θ a unit vector pointing θ from the $-z$ axis (see Fig. 1), the Ramsey protocol corresponds to a quench from $h = \infty$ to $h = 0$. One may therefore be able to explore, e.g., Kibble-Zurek physics [52, 53].

Theoretical methods.—We calculate dynamics in four limits: (1) short times, $\{J_{\perp}, J_z\}t \ll 1$, (2) Ising, $J_{\perp} = 0$, (3) near-Heisenberg [SU(2)], $|J_z - J_{\perp}| \ll J_z$, and (4) one dimension for arbitrary J_{\perp}/J_z . We develop analytic tools in arbitrary dimension for limits (1-3) and study (4) with the numerically exact adaptive time-dependent density matrix renormalization group (t-DMRG) [54–57]. All are obtained by time-evolving under Eq. (1)’s H , corresponding to the middle leg of the Ramsey spectroscopy. We will present calculational details elsewhere [40]. In all cases $\langle S_j^z \rangle = -(f/2) \cos \theta$ is conserved.

Short time limit, $\{J_{\perp}, J_z\}t \ll 1$. For short times,

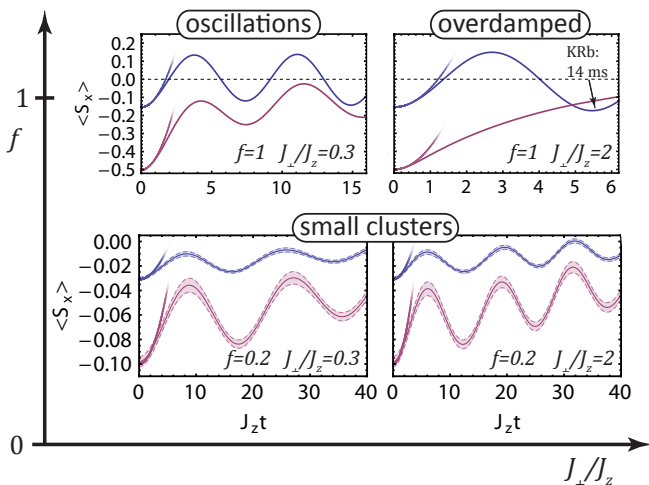


FIG. 3. (Color online) “Phase diagram” illustrating crossovers of dynamics versus filling f , J_{\perp}/J_z , and θ using t-DMRG on chains. In each region, a plot shows dynamics for $\theta = 0.1\pi, 0.5\pi$ (top blue, bottom purple), labeled with a qualitative description. Shaded regions for $f = 0.2$ indicate one standard deviation from disorder averaging 100 configurations. The partial curves at short times are obtained from our perturbative expansions, Eqs. (2). “KRb: 14 ms” indicates the time for KRb in a 5 kV/cm dc \mathbf{E} -field, using $|0\rangle$ and $|1\rangle$ as the spin-1/2 (see Fig. 2). Dynamics in higher dimensions is faster due to having more neighbors.

$\langle \mathcal{O}(t) \rangle = \langle \mathcal{O} \rangle - it \langle [\mathcal{O}, H] \rangle - \frac{t^2}{2} \langle [[\mathcal{O}, H], H] \rangle + O(t^3)$ for an observable \mathcal{O} . We calculate the commutators and time dependence of $\langle S^{\alpha}(t) \rangle$ to leading non-zero order, and $\langle S^{\alpha}(t) S^{\gamma}(t) \rangle$ to linear order. We find

$$\begin{aligned} \langle S_i^x \rangle &= \frac{f}{2} \sin \theta \left\{ 1 - \frac{f\tau^2}{8} [\Xi_2 + f\Upsilon \cos^2 \theta] \right\} + O(\tau^4), \\ \langle S_i^y \rangle &= -(f^2 \tau \Xi_1 / 8) \sin(2\theta) + O(\tau^3), \end{aligned} \quad (2)$$

where $\tau = (J_z - J_{\perp})t$, $\Xi_m = \sum_{j \neq 0} V_{dd}^m(i, i+j)$, and $\Upsilon = \Xi_1^2 - \Xi_2$. Note that for these homogeneous systems, these observables are independent of i . Similarly, defining $\mathcal{C}_{ij}^{\alpha\gamma} \equiv \langle S_i^{\alpha} S_j^{\gamma} \rangle$, we find

$$\begin{aligned} \mathcal{C}_{ij}^{xy} &= \frac{\tau f^3 \sin(2\theta) \sin \theta}{16} [V_{dd}(i, j) - \Xi_1] + O(\tau^2) \\ \mathcal{C}_{ij}^{yz} &= \frac{\tau f^3}{8} \left[\frac{\sin(2\theta) \cos \theta}{2} \Xi_1 + V_{dd}(i, j) \sin^3 \theta \right] + O(\tau^2) \end{aligned} \quad (3)$$

for $i \neq j$. To linear order, $\mathcal{C}_{ij}^{\alpha\alpha}$ and $\mathcal{C}_{ij}^{\alpha\gamma}$ are constant. For $i = j$, the Pauli algebra reduces $\langle S_i^{\alpha} S_i^{\gamma} \rangle$ to $\langle S_i^{\delta} \rangle$. One can compute Ξ_m rapidly for arbitrary lattices and analytically in special cases (e.g. one dimension).

Ising limit, $J_{\perp} = 0$. We extend the Emch-Radin solution [58–62] for Ising dynamics to arbitrary θ , interspin coupling strengths, correlations, and to include disorder [63]. We find

$$\langle S_i^x(t) \rangle = f \frac{\sin(\theta)}{2} \text{Re} \left[\prod_{j \neq i} \sum_{\rho_j} g(\rho_j) e^{\frac{1}{2} i t J_z V_{dd}(i, i+j) \rho_j} \right], \quad (4)$$

where the sum runs over $\rho = 0$ (unoccupied site) and $\rho = \pm 1$ ($S^z = \pm 1/2$), and $g(\rho) = (1-f)\delta_{\rho,0} + f \sin^2(\theta/2)\delta_{\rho,1} + f \cos^2(\theta/2)\delta_{\rho,-1}$. The expectation $\langle S_i^y \rangle$ takes the imaginary (rather than real) part of the square-bracketed expression in Eq. (4). Similarly one can obtain correlations [40]. The product in Eq. (4) is readily evaluated numerically by truncating the interaction range, even for a truncation including thousands of sites. In special limits $\langle S_i^x \rangle$ simplifies: e.g., for $\theta = \pi/2$ and $f = 1$, $\langle S_i^x(t) \rangle = (1/2) \prod_{j \neq i} \cos(J_z V_{dd}(i, j)t/2)$.

Near-Heisenberg limit, $J_z \approx J_{\perp}$.—Here a finite size gap $\Delta \propto J_{\perp}/N^2$ for N particles to excitations out of the Dicke (fully symmetric) manifold prevents states initially in the manifold from leaving it when $|J_z - J_{\perp}| \ll \Delta$ [64, 65]. The effective Hamiltonian obtained from projecting H to the Dicke manifold is the collective spin $N/2$ model [64, 65] $H_{\text{eff}} = \chi(S^z)^2$ with $\chi = \frac{J_{\perp} - J_z}{N(N-1)} \sum_{i \neq j} V_{dd}(i, i+j)$. Dynamics are straightforwardly calculated for any disorder configuration, since there are only $N+1$ states in the Dicke manifold; for example $\langle S_i^x \rangle = \frac{\sin \theta}{2} \text{Re} \left[(\cos(\chi\tau) - i \cos \theta \sin(\chi\tau))^{N-1} \right]$. Again $\langle S_i^y \rangle$ is the corresponding imaginary part. Unlike the other approximations, this is valid only for finite N .

One dimension.—We use adaptive t-DMRG [54–57] to calculate dynamics of one dimensional chains. We treat 20 site chains and find finite size effects to be fairly small. We discretize time in steps of $0.05J_z^{-1}$, and find a discarded weight of $\lesssim 10^{-9}$ for times $\lesssim 10J_z^{-1}$, adaptively keeping $m = 50$ -500 reduced density matrix states. Altogether, we expect errors dominated by the disorder average, which is taken over 100 random configurations.

Results: global perspective.—Fig. 3 overviews dynamics, from the calculations above, as a function of J_{\perp}/J_z , f , and θ . Experimentally, these are controlled by electric field [26, 27], temperature/density, and first Ramsey pulse area, respectively. Fig. 3 presents dimension $d = 1$ results, but our analytic expressions show that the $d = 1$ results are representative of $d > 1$. Dynamics in $d > 1$ has more neighbors and thus is faster. Fig. 3 shows that the short time expansion describes the dynamics to a time at which $\langle S^x(t) \rangle$ changes from $\langle S^x(t=0) \rangle$ by more than the disorder fluctuations (shaded regions), enabling experiments to measure the short time dynamics “signal” above the disorder “noise.”

Next, consider $f = 1$ and $\theta = \pi/2$. For $J_{\perp}/J_z = 0$, $\langle S_i^x \rangle$ oscillates with period $2\pi/J_z$ from the nearest neighbor interaction, superposed with slower oscillations from longer range interactions. The first-few-neighbor interactions account for the dynamics to times $t \sim 10J_z^{-1}$. For $J_{\perp} = 0$ the frequencies form a discrete set. Increasing J_{\perp} gives a continuum of frequencies, damping the oscillations. Approaching $J_{\perp} = J_z$, the dynamics slows down, since at $J_{\perp} = J_z$ the initial state is an eigenstate of the Hamiltonian. As J_{\perp}/J_z increases further, the dynamics is damped with characteristic timescale $(J_{\perp} - J_z)^{-1}$.

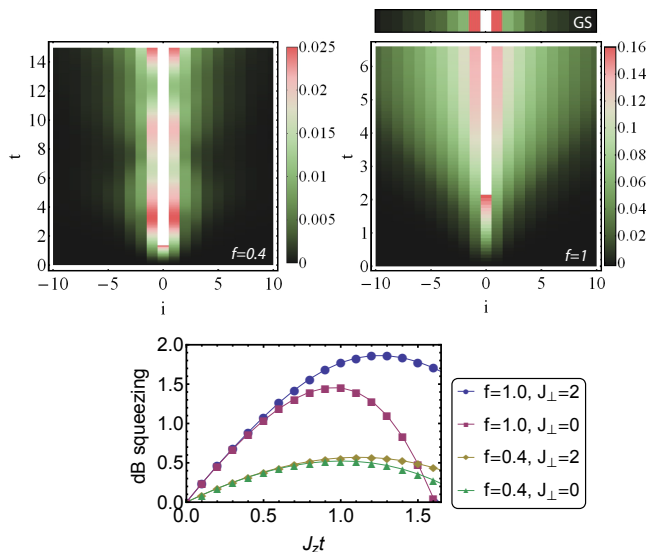


FIG. 4. (Color online) Correlation and squeezing dynamics. Top: $\langle S_j^x S_{j+i}^x \rangle - \langle S_j^x \rangle \langle S_{j+i}^x \rangle$ (averaged over j) for $J_\perp = 2J_z$ with $\theta = \pi/2$ as a function of time for $f = 0.4$ (left) and $f = 1$ (right), compared to the ground state (upper right bar). Other f , θ , and J_\perp are similar. Bottom: squeezing in decibels as a function of time, quantifying quantum-enhanced metrological utility, for $J_\perp = 2J_z, f = 1$; $J_\perp = 0, f = 1$; $J_\perp = 2J_z, f = 0.4$, and $J_\perp = 0, f = 0.4$ (top to bottom) and $\theta = \pi/2$.

For $f \ll 1$, the behavior crosses over to that of independent clusters, eventually with only two particles. The largest frequency is roughly half that for $f = 1$, since there is a single neighbor instead of two. Thus, the dynamics remains roughly as fast as for $f = 1$, but the dynamics' magnitude at times $\sim \{J_z^{-1}, J_\perp^{-1}\}$ is smaller since there are fewer molecules and only a fraction of them are close enough to interact. At any f the overall timescales are roughly independent of θ , but for small θ or to linear order in time, the Bloch vector undergoes roughly mean-field precession, while for $\theta \approx \pi/2$ or longer times, it depolarizes (shrinks).

Achieving goals of emulating quantum magnetism.—For experimental verification of the emulation of the XXZ model and benchmarking of its accuracy, we consider short time dynamics. Fig. 2 (right) shows their characteristic dependence on θ , f , and $\{J_z, J_\perp\}$. Fig. 2 (left) shows J_z and J_\perp 's dependence on the dc electric field for two rotational state choices.

To achieve the second goal of generating interesting well-understood states, we note that for $f \approx 1$ and $\theta = \pi/2$ and $J_z \approx J_\perp$, the state at $t = \pi/(2\chi)$ is $|GHZ\rangle = (1/\sqrt{2})(|\leftarrow \dots \leftarrow\rangle + e^{i\phi} |\rightarrow \dots \rightarrow\rangle)$ for some ϕ [64–67]. This is a cat state, specifically GHZ/NOON state, useful for metrology [68]. Ising dynamics offer other interesting states. For nearest neighbor interactions and $\theta = \pi/2$, the state at $t = \pi/(2J_z)$ is a cluster state, which suffices for universal measurement based

quantum computing [69].

Figure 4 (bottom) quantifies how one notion of the utility of these quantum states – their ability to perform quantum-enhanced metrology – extends to $f < 1$. While the precision of measuring frequencies with uncorrelated spins is limited to the standard quantum limit, scaling as $1/\sqrt{N}$, entangled spins with “squeezing” can scale as $1/N$. The squeezing parameter ξ quantifies this improvement, given by $\xi \equiv \min_{\hat{n}_\phi} \frac{\sqrt{N} \sqrt{\langle (S \cdot \hat{n}_\phi)^2 \rangle - \langle S \cdot \hat{n}_\phi \rangle^2}}{\langle S^x \rangle}$ minimizing over unit vectors \hat{n}_ϕ in the y - z plane. For $\theta = \pi/2$, Fig. 4 (bottom) plots decibels squeezing, dB squeezing = $-10 \log_{10} \xi$, for 100 independent tubes with $L = 20$. It shows that substantial squeezing (dB squeezing > 0) occurs for a broad range of J_\perp/J_z and t , even if $f < 1$. In fact, it appears squeezing generically persists for all f .

A generic implementation of the proposed dynamics in $d > 1$ achieves the third goal, emulating quantum magnetism in theoretically intractable regimes. Away from the short time, Ising, and Heisenberg limits, no solution is known in $d > 1$. As Fig. 4 shows, in $d = 1$ strong correlations develop. For $f = 1$ these are even larger at large distance than in the ground state. Interestingly, the dynamics shows a light-cone-like spreading to an apparent steady state. We note recent work on many-body localization in quenches of disordered XXZ chains [70].

Experimental outlook.—Though our discussion focused on molecules, we point out that the dynamics studied here can have direct application in other physical systems, including condensed matter [48], trapped ions [51, 71], and optical lattice clocks [72, 73].

We close by noting technical details for molecule experiments. Rotational states' polarizabilities differ [26, 74], so the optical trap induces a spatially varying field $\sum_i h_i S_i^z$. Also, Eq. (1) ignores density-density $n_i n_j$ and density-spin $n_i S_j^z$ interactions [26, 27]. For $f < 1$, the latter gives a spatially varying magnetic field that depends on molecules' random positions. Spin-echo pulses common in Ramsey experiments remove both effects.

Summary.—We have shown that Ramsey spectroscopy enables ongoing ultracold polar molecule experiments to accomplish three goals for emulating quantum magnetism: (1) benchmarking the emulation's accuracy (using short time dynamics), (2) generating strongly correlated and entangled states in well-understood limits (Ising, near-Heisenberg, one dimension), and (3) exploring strongly correlated dynamics in regimes inaccessible to theory (generic case in dimensions $d > 1$).

Finally, we mention that in addition to the XXZ Hamiltonian explored in this paper, our dynamic protocol should be useful for verifying emulation of more complicated spin models that may be realized with ultracold molecules, as in Refs. [25–27] and beyond.

Acknowledgements.—We thank A. Gorshkov, J. Bollinger, M. Kastner, M. Lukin, J. Ye, D. Jin, and the Jin-Ye molecule group for numerous conversations. KH

thanks the NRC for support and the Aspen Center for Physics, which is supported by the NSF, for its hospitality during the initial conception of this work. This work utilized the Janus supercomputer, which is supported by the NSF (award number CNS-0821794) and the University of Colorado Boulder, and is a joint effort with the University of Colorado Denver and the National Center for Atmospheric Research. AMR acknowledges support from the NSF (PFC and PIF), ARO individual investigator award and ARO with funding for the DARPA-OLE program. This manuscript is the contribution of NIST and is not subject to U.S. copyright.

* kaden.hazzard@colorado.edu

- [1] K. Ni, S. Ospelkaus, M. H. G. de Miranda, A. Pe'er, B. Neyenhuis, J. J. Zirbel, S. Kotochigova, P. S. Julienne, D. S. Jin, and J. Ye, *Science* **322**, 231 (2008).
- [2] S. Ospelkaus, K.-K. Ni, G. Quémener, B. Neyenhuis, D. Wang, M. H. G. de Miranda, J. L. Bohn, J. Ye, and D. S. Jin, *Phys. Rev. Lett.* **104**, 030402 (2010).
- [3] S. Ospelkaus, K.-K. Ni, D. Wang, M. H. G. de Miranda, B. Neyenhuis, G. Quémener, P. S. Julienne, J. L. Bohn, D. S. Jin, and J. Ye, *Science* **327**, 853 (2010).
- [4] K.-K. Ni, S. Ospelkaus, D. Wang, G. Quémener, B. Neyenhuis, M. H. G. de Miranda, J. L. Bohn, J. Ye, and D. S. Jin, *Nature* **464**, 1324 (2010).
- [5] M. H. G. de Miranda, A. Chotia, B. Neyenhuis, D. Wang, G. Quémener, S. Ospelkaus, J. L. Bohn, J. Ye, and D. S. Jin, *Nature Physics* **7**, 502 (2011).
- [6] A. Chotia, B. Neyenhuis, S. A. Moses, B. Yan, J. P. Covey, M. Foss-Feig, A. M. Rey, D. S. Jin, and J. Ye, *Phys. Rev. Lett.* **108**, 080405 (2012).
- [7] T. Zelevinsky, S. Kotochigova, and J. Ye, *Phys. Rev. Lett.* **100**, 043201 (2008).
- [8] D. DeMille, *Phys. Rev. Lett.* **88**, 067901 (2002).
- [9] L. D. Carr, D. DeMille, R. V. Krems, and J. Ye, *New Journal of Physics* **11**, 055049 (2009).
- [10] T. Lahaye, C. Menotti, L. Santos, M. Lewenstein, and T. Pfau, *Reports on Progress in Physics* **72**, 126401 (2009).
- [11] C. Trefzger, C. Menotti, B. Capogrosso-Sansone, and M. Lewenstein, *Journal of Physics B: Atomic, Molecular and Optical Physics* **44**, 193001 (2011).
- [12] M. A. Baranov, M. Dalmonte, G. Pupillo, and P. Zoller, arxiv:1207.1914v1 .
- [13] R. Barnett, D. Petrov, M. Lukin, and E. Demler, *Phys. Rev. Lett.* **96**, 190401 (2006).
- [14] A. Micheli, G. Brennen, and P. Zoller, *Nature Physics* **2**, 341 (2006).
- [15] H. P. Büchler, A. Micheli, and P. Zoller, *Nature Physics* **3**, 726 (2007).
- [16] T. Watanabe, *Phys. Rev. A* **80**, 053621 (2009).
- [17] M. L. Wall and L. D. Carr, *New Journal of Physics* **11**, 055027 (2009).
- [18] H. Yu, W. M. Liu, and C. Lee, arXiv:0910.4922 .
- [19] *Cold molecules: Creation and applications*, edited by R. V. Krems, B. Friedrich, and W. C. Stwalley (Taylor & Francis, 130 Milton Park, Abingdon, Oxon OX14 4SB, UK, 2008).
- [20] M. L. Wall and L. D. Carr, *Phys. Rev. A* **82**, 013611 (2010).
- [21] J. Schachenmayer, I. Lesanovsky, A. Micheli, and A. J. Daley, *New Journal of Physics* **12**, 103044 (2010).
- [22] J. Pérez-Ríos, F. Herrera, and R. V. Krems, *New Journal of Physics* **12**, 103007 (2010).
- [23] C. Trefzger, M. Alloing, C. Menotti, F. Dubin, and M. Lewenstein, *New Journal of Physics* **12**, 093008 (2010).
- [24] J. P. Kestner, B. Wang, J. D. Sau, and S. Das Sarma, *Phys. Rev. B* **83**, 174409 (2011).
- [25] S. R. Manmana, E. M. Stoudenmire, K. R. A. Hazzard, A. M. Rey, and A. V. Gorshkov, arXiv:1210.5518 .
- [26] A. V. Gorshkov, S. R. Manmana, G. Chen, J. Ye, E. Demler, M. D. Lukin, and A. M. Rey, *Phys. Rev. Lett.* **107**, 115301 (2011).
- [27] A. V. Gorshkov, S. R. Manmana, G. Chen, E. Demler, M. D. Lukin, and A. M. Rey, *Phys. Rev. A* **84**, 033619 (2011).
- [28] A. Auerbach, *Interacting electrons and quantum magnetism* (Springer-Verlag, New York, 1994).
- [29] S. Sachdev, *Nature Physics* **4**, 173 (2008).
- [30] *Introduction to frustrated magnetism*, edited by C. Lacroix, P. Mendels, and F. Mila (Springer, Heidelberg, 2011).
- [31] I. Bloch, J. Dalibard, and W. Zwerger, *Rev. Mod. Phys.* **80**, 885 (2008).
- [32] B. Neyenhuis, B. Yan, S. A. Moses, J. P. Covey, A. Chotia, A. Petrov, S. Kotochigova, J. Ye, and D. S. Jin, arxiv:1209.2226 .
- [33] The electric field ensures that the two rotational levels are sufficiently off-resonant from other levels that they form an isolated spin-1/2 [27].
- [34] We neglect hyperfine coupling, as Refs. [26, 27] justify.
- [35] J. Deiglmayr, A. Grochola, M. Repp, K. Mörtlbauer, C. Glück, J. Lange, O. Dulieu, R. Wester, and M. Weidemüller, *Phys. Rev. Lett.* **101**, 133004 (2008).
- [36] S. Trotzky, P. Cheinet, S. Fölling, M. Feld, U. Schnorrberger, A. M. Rey, A. Polkovnikov, E. A. Demler, M. D. Lukin, and I. Bloch, *Science* **319**, 295 (2008).
- [37] D. Jin and J. Ye, private communication.
- [38] In addition to simplicity, this disorder distribution results from suddenly quenching tunneling t to zero for lattice fermions initially at a temperature $T \gg t$.
- [39] T. Takekoshi, M. Debatin, R. Rameshan, F. Ferlaino, R. Grimm, H.-C. Nägerl, C. R. Le Sueur, J. M. Hutson, P. S. Julienne, S. Kotochigova, and E. Tiemann, *Phys. Rev. A* **85**, 032506 (2012).
- [40] K. R. A. Hazzard, S. R. Manmana, M. Foss-Feig, and A. Maria, in preparation .
- [41] G. Aeppli, H. Guggenheim, and Y. J. Uemura, *Phys. Rev. Lett.* **52**, 942 (1984).
- [42] C. Kraemer, N. Nikseresht, J. O. Piatek, N. Tsyrlin, B. D. Piazza, K. Kiefer, B. Klemke, T. F. Rosenbaum, G. Aeppli, C. Gannarelli, K. Prokes, A. Podlesnyak, T. Strössle, L. Keller, O. Zaharko, K. W. Krämer, and H. M. Rønnow, *Science* **336**, 1416 (2012).
- [43] M. Blume, V. J. Emery, and R. B. Griffiths, *Phys. Rev. A* **4**, 1071 (1971).
- [44] R. B. Griffiths, *Phys. Rev. Lett.* **23**, 17 (1969).
- [45] Y. Gefen, A. Aharony, and S. Alexander, *Phys. Rev. Lett.* **50**, 77 (1983).
- [46] C. L. Henley, *Phys. Rev. Lett.* **54**, 2030 (1985).
- [47] M. Randeria, J. P. Sethna, and R. G. Palmer, *Phys. Rev. Lett.* **54**, 1321 (1985).
- [48] J. A. Quilliam, S. Meng, and J. B. Kycia, *Phys. Rev. B*

- 85**, 184415 (2012).
- [49] K. Trinh, S. Haas, R. Yu, and T. Roscilde, *Phys. Rev. B* **85**, 035134 (2012).
- [50] K. R. A. Hazzard, A. V. Gorshkov, and A. M. Rey, *Phys. Rev. A* **84**, 033608 (2011).
- [51] J. W. Britton, B. C. Sawyer, A. C. Keith, C.-C. J. Wang, J. K. Freericks, H. Uys, M. J. Biercuk, and J. J. Bollinger, *Nature* **484**, 489 (2012).
- [52] T. W. B. Kibble, *Journal of Physics A: Mathematical and General* **9**, 1387 (1976).
- [53] W. H. Zurek, *Nature* **317**, 505 (1985).
- [54] S. R. White, *Phys. Rev. Lett.* **69**, 2863 (1992).
- [55] G. Vidal, *Phys. Rev. Lett.* **93**, 040502 (2004).
- [56] A. J. Daley, C. Kollath, U. Schollwöck, and G. Vidal, *J. Stat. Mech.* P04005 (2004).
- [57] U. Schollwöck, *Rev. Mod. Phys.* **77**, 259 (2005).
- [58] G. G. Emch, *Journal of Mathematical Physics* **7**, 1198 (1966).
- [59] C. Radin, *Journal of Mathematical Physics* **11**, 2945 (1970).
- [60] M. Kastner, *Phys. Rev. Lett.* **106**, 130601 (2011).
- [61] M. Foss-Feig, K. R. A. Hazzard, J. J. Bollinger, and A. M. Rey, arXiv:1209.5795 .
- [62] M. van den Worm, B. C. Sawyer, J. J. Bollinger, and M. Kastner, arXiv:1209.3697 .
- [63] These results also extend straightforwardly to arbitrary spatially varying initial angles and longitudinal magnetic fields, as we present elsewhere [40].
- [64] A. M. Rey, L. Jiang, M. Fleischhauer, E. Demler, and M. D. Lukin, *Phys. Rev. A* **77**, 052305 (2008).
- [65] R. M. Rajapakse, T. Bragdon, A. M. Rey, T. Calarco, and S. F. Yelin, *Phys. Rev. A* **80**, 013810 (2009).
- [66] K. Mølmer and A. Sørensen, *Phys. Rev. Lett.* **82**, 1835 (1999).
- [67] X. Wang, A. S. Sørensen, and K. Mølmer, *Phys. Rev. A* **64**, 053815 (2001).
- [68] J. J. . Bollinger, W. M. Itano, D. J. Wineland, and D. J. Heinzen, *Phys. Rev. A* **54**, R4649 (1996).
- [69] R. Raussendorf and H. J. Briegel, *Phys. Rev. Lett.* **86**, 5188 (2001).
- [70] J. H. Bardarson, F. Pollmann, and J. E. Moore, *Phys. Rev. Lett.* **109**, 017202 (2012).
- [71] K. Kim, M.-S. Chang, S. Korenblit, R. Islam, E. Edwards, J. Freericks, G.-D. Lin, L.-M. Duan, and C. Monroe, *Nature* **465**, 590 (2010).
- [72] M. D. Swallows, M. Bishof, Y. Lin, S. Blatt, M. J. Martin, A. M. Rey, and J. Ye, *Science* **331**, 1043 (2011).
- [73] N. D. Lemke, J. von Stecher, J. A. Sherman, A. M. Rey, C. W. Oates, and A. D. Ludlow, *Phys. Rev. Lett.* **107**, 103902 (2011).
- [74] S. Kotochigova and D. DeMille, *Phys. Rev. A* **82**, 063421 (2010).